

# A van der Waals density functional mapping of attraction in DNA dimers

Elisa Londero, Per Hyldgaard, and Elsebeth Schröder\*

*Microtechnology and Nanoscience, MC2, Chalmers University of Technology, SE-412 96 Göteborg, Sweden*

(Dated: April 6, 2013)

The dispersion interaction between a pair of parallel DNA double-helix structures is investigated by means of the van der Waals density functional (vdW-DF) method. Each double-helix structure consists of an infinite repetition of one B-DNA coil with 10 base pairs. This parameter-free density functional theory (DFT) study illustrates the initial step in a proposed vdW-DF computational strategy for large biomolecular problems. The strategy is to first perform a survey of interaction geometries, based on the evaluation of the van der Waals (vdW) attraction, and then limit the evaluation of the remaining DFT parts (specifically the expensive study of the kinetic-energy repulsion) to the thus identified interesting geometries. Possibilities for accelerating this second step is detailed in a separate study. For the B-DNA dimer, the variation in van der Waals attraction is explored at relatively short distances (although beyond the region of density overlap) for a 360° rotation. This study highlights the role of the structural motifs, like the grooves, in enhancing or reducing the vdW interaction strength. We find that to a first approximation, it is possible to compare the DNA double strand at large wall-to-wall separations to the cylindrical shape of a carbon nanotube (which is almost isotropic under rotation). We compare our first-principles results with the atom-based dispersive interaction predicted by DFT-D2 [J. Comp. Chem. **27**, 1787 (2006)] and find agreement in the asymptotic region. However, we also find that the differences in the enhancement that occur at shorter distances reveal characteristic features that result from the fact that the vdW-DF method is an electron-based (as opposed to atom-based) description.

## I. INTRODUCTION

The key characteristics of a working biomolecular system is an enormous richness of structural complexity and a robust working principle, molecular recognition, for identifying geometries that optimize the intermolecular binding and alignment. Stronger covalent or ionic binding determines the structure inside the molecules and provides resilience towards statistical fluctuations.<sup>1</sup> This permanence is, for example, of utmost importance in the preservation of the information contained in our deoxyribonucleic acid (DNA) genome.<sup>2,3</sup> The binding that is of relevance for life processes, e.g., the molecular-recognition matching<sup>4-6</sup> of genes, is weaker to allow the reversible operations that Nature needs.<sup>1</sup> The molecular recognition arises as a delicate balance between steric hindrance, electrostatics, and van der Waals (vdW) attraction, the latter also termed the London dispersion interaction.

The search for a deeper understanding of such biomolecular operation motivates development of a parameter-free computational theory that both provides transferability and computational efficiency.<sup>7,8</sup> The structural complexity of the biomolecular systems implies that the supramolecular system may express itself in a multitude of ways, and it is not certain that a given empirical (or semi-empirical) interaction model remains applicable for all emerging configurations and for varying charging states.

Density Functional Theory (DFT) is a highly valued condensed-matter theory tool that is our work horse in predictive computational theory of traditional materials problems.<sup>9</sup> In such systems, the electron density remains high between the atoms, for example, in a bulk structure.

DFT also works excellently for individual molecules but it has until recently lacked an account of the truly nonlocal correlations that underpin vdW interactions between constituents in a molecular system. The issue is that molecular systems are inherently sparse:<sup>10-12</sup> they must also contain low electron-density regions between the molecular fragments. The sparseness is even the defining quality when Nature puts molecular recognition to work among biomolecules. Nevertheless, the last decade have seen developments that position DFT to overcome this previous limitation.

The vdW density functional (vdW-DF) method<sup>13-15</sup> has a track record<sup>12</sup> as a general-purpose nonempirical DFT that can characterize interactions in sparse and soft biomolecular systems. The vdW-DF method accounts for vdW interactions by introducing true nonlocality in the density functional. Being built as a physics-based description and within a constraint-based design, it has the electron-based description that helps transferability. This is, for example, important for systems where it is essential to describe the vdW binding or attraction for several typical separations.<sup>16-18</sup> This is true even if the plasmon-type description may not capture the full complexity in the description of the far-apart-regime for some systems that effectively behave as a low-dimensional metal.<sup>19-21</sup> There exist efficient implementations also for self-consistent evaluations. One such algorithm<sup>22</sup> uses a fast Fourier transform approach which accelerates evaluation for medium-to-large size systems while real-space evaluation approaches<sup>17,23-26</sup> may hold advantages for very-large-scaled systems, as discussed in Ref. 17.

This paper reports that a nonempirical vdW-DF characterization of the variation in the vdW attraction among biopolymers is indeed feasible. In vdW-DF, this vdW

attraction is reflected in a nonlocal correlation term  $E_c^{\text{nl}}$ . Other terms, including a single-particle kinetic energy term  $T_s$  and the semilocal parts of the exchange-correlation energy  $E_{xc}^0$  also contribute to the vdW-DF total energy  $E_{\text{tot}}^{\text{vdW-DF}}$  but (for objects that are effectively neutral) it is the vdW attraction, contained in  $E_c^{\text{nl}}$ , that dominates when the density overlap between fragments can be ignored. Our vdW-DF characterization presented here thus computes the  $E_c^{\text{nl}}$  variation to map the morphology dependence in the vdW attraction between a pair of parallel, infinitely-repeated double-stranded (ds) DNA helices. We find that the vdW interaction of such DNA dimer is sensitive to the alignment of the major DNA structural motifs, particularly different orientations of the major and minor grooves of the two ds-DNA macromolecules. We also identify and discuss a set of systematic changes that arise in the vdW attraction when the problem is investigated across a range of interaction distances.<sup>16,27</sup> We further compare the  $E_c^{\text{nl}}$  variation to the evaluation of the semiempirical vdW term of a vdW-extended DFT method,<sup>28</sup> namely DFT-D2.<sup>29</sup> We use and extend analytical interaction results<sup>30–32</sup> that apply for the far (but not asymptotically far) regime, to illustrate the difference in nature between our electron-based vdW-DF study and the atom-based DFT-D approach. Moreover, we contrast this interpretation of the vdW attraction in a DNA dimer with corresponding results for a dimer of carbon nanotubes (CNTs).

With this study we propose a vdW-DF computational strategy for large-biomolecules, the strategy *begins* non-empirical studies of the interactions by a mapping of the vdW-attraction term  $E_c^{\text{nl}}$ . This is suggested to optimize computational efficiency. We observe that the  $E_c^{\text{nl}}$  mapping of vdW attraction can today be carried out at the cost of about ten wall time minutes per DNA dimer interaction geometry. That is much smaller than the time it takes to evaluate the variation in the kinetic energy  $T_s$  because of an excellent scaling of real-space evaluations of  $E_c^{\text{nl}}$ , Ref. 17. The cost of computing  $T_s$  through wavefunctions is the same for DFT-D and vdW-DF so our suggested strategy could also be relevant, for example, for large-system DFT-D studies.<sup>28,29</sup> The motivation for our proposal is that a complete nonempirical vdW-DF evaluation can be focused on the relevant interaction morphologies that the  $E_c^{\text{nl}}$  mapping identifies. The possibilities for using an adapted Harris scheme<sup>33–36</sup> to accelerate the complete vdW-DF evaluation is discussed and assessed in a closely related publication, Ref. 18.

The paper is organized as follows. The ds-DNA and DNA dimer systems are described and discussed in Section II, which also introduces the particular CNT structure investigated here. In Section III we present the computational method used. Section IV consists of a study of the nonlocal correlation energy variation as the distance between the DNAs is changed and the two structures are rotated. It also contains comparisons of our vdW-DF-based results in the far (nearly asymptotic) region to the dispersion interaction predicted by DFT-D2,<sup>29</sup> and with

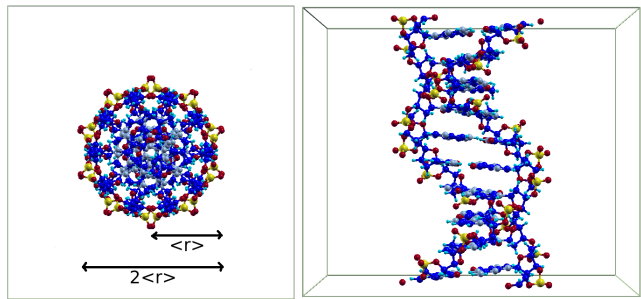


FIG. 1: Along-axis and side views of a minimal repeat-unit cell model of the ds-DNA macromolecule. The atoms are P (yellow), O (dark red), H (cyan), N (blue), and C (gray). Figure created using XCRYSDEN.<sup>37</sup>

results of similar studies for CNTs.

## II. GENOME STRUCTURE, A DNA MODEL

The primary structure of DNA is made up by four different nucleobases, the adenine (A), guanine (G), cytosine (C) and thymine (T) bases, each covalently linked to a sugar. These building blocks are joined to a strand by phosphate groups connecting the sugars. The two DNA strands form a double helix with (predominantly) hydrogen bonds linking base pairs, thus forming the DNA secondary structure. The repeated pairing between a purine base (A or G) and a smaller pyrimidine (T or C) produces a constant diameter for the double helix.

One of us was previously involved in a vdW-DF study of the nucleobases, focusing on the stacking interactions.<sup>7</sup> Even if the vdW forces by themselves may have limited selectivity (for small molecules like base pairs), the vdW forces are essential in the building of this secondary structure because they drive, optimize, and hold a structural assembly until more stable bonds can be formed. This mechanism is fundamental in the case of molecular recognition and in DNA replication. The previous study<sup>7</sup> provides vdW-DF analysis and results for the Rise and Twist of the base pairs inside (that is, between the backbones of) the ds-DNA structure. The nonlocal correlation contribution  $E_c^{\text{nl}}$  to vdW-DF will by itself have difficulties in aligning small molecules but the vdW forces still position these components (base pairs) close enough that the corrugation from kinetic-energy repulsion is expressed. The previous vdW-DF study<sup>7</sup> reported a very good agreement between vdW-DF characterizations and experimental information (for example, correlations in base-pair rotation angles as extracted from the Nucleic Acid Database<sup>3</sup>). This progress highlights possibilities of a broader application of the vdW-DF method to soft matter challenges and in particular to refine the description of the vdW attraction between biopolymers.

We focus our large-scale vdW-DF interaction study on dimers of a ds-DNA model structure in the B-form.

Both ds-DNA fragments are assumed to have the periodically repeated sequence of nucleobases GCAATACGGT. The ds-DNA atomic structure is built from idealized coordinates.<sup>38–40</sup> In our model the axes of the two ds-B-DNA fragments are straight and parallel to each other.

Figure 1 shows the atomic positions in the minimal-repeat unit cell for one ds-B-DNA molecule. On the most coarse level it reflects a cylinder-like form for DNA but it also shows both major and minor grooves of the double helix. This DNA model contains 635 atoms and is limited to one coil, but it is periodic and is used as the repeat unit cell of a DFT calculation so that the DNA is still described as a macromolecular system (through the infinite repetition of the unit cell along the DNA axis).

The polar sugar-phosphate strand on the external part of the chain can form favorable interactions with ions in a solvent. Each phosphate group then carries a negative charge which is balanced by positive ions, the counter ions, in the surrounding liquid. The counter ions stabilize the structure, making the DNA-ion system charge neutral. Correlation between the concentrations in the counter ions may themselves contribute further to an attraction between the DNA-ion system and another organic molecule. However, we shall not consider such effects here. Instead we investigate the vdW binding arising from nonlocal electron correlation effects between two ds-DNA structures assuming (and enforcing in our DFT calculations) that the DNA repeated-unit cell model structure itself remains charge neutral. A forthcoming study addresses the effects on the vdW attraction of the charging by counter ions.

The double-helix structure is very regular, and when viewed along the axis appears almost isotropic (left panel of Fig. 1). This average isotropy of DNA simplifies our study of the sensitivity of the vdW binding to macromolecular structural motifs. The average isotropy also helps in the comparison with CNT dimer interactions as we can define an approximate “radius” of DNA. We can thus compare the vdW interactions as a function of wall-to-wall distances  $\Delta$  in dimers of DNA and dimers of CNT, using the analysis of Refs. 27,30–32. For DNA we use the radius that is defined as the average of the helix backbone P and O atoms distances from the DNA center (8.5 Å and 9.7 Å). This yields the approximate DNA radius  $\langle r \rangle_{\text{DNA}} \approx 9.1$  Å (shown by a double-arrow line in Figure 1), close to that of the standard literature description where the diameter is taken to be  $\approx 20$  Å. For a given center-to-center separation  $d$  of the DNA dimer structure we thus use  $\Delta = d - 2\langle r \rangle_{\text{DNA}}$  as the wall-to-wall separation of the DNA dimer.

The approximate similarity of DNA with the cylinder form of a CNT represents one major structural motif of the structure. Another major structural motif is obviously the existence of grooves (right panel), a feature which is distinctly different from what characterizes the CNTs.

The systems studied here are sparse<sup>12</sup> so that the vdW interaction (with electrostatics) dominates in the inter-

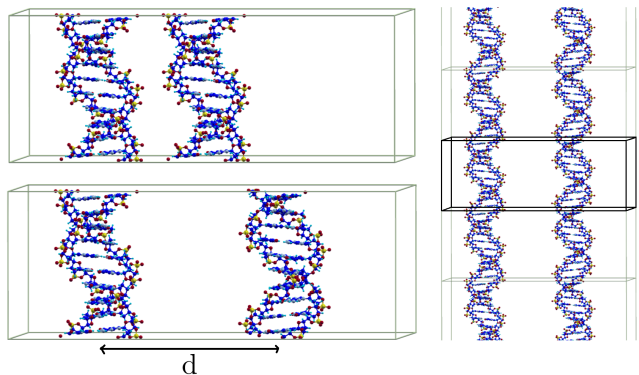


FIG. 2: Left: Example of a system obtained starting from a single 33.8 Å period of the ds-DNA that is copied, translated and rotated inside an enlarged unit cell. Right: Portion of the final system studied. Here we have piled a number of unit cells (not all shown) on top of each other in preparation of the real-space evaluation of Eq. (2). Figure created using XCRYSDEN.<sup>37</sup>

molecular regions of low electron density. By basing the function on weaker forces, Nature ensures a truly remarkable resilience of our genetic code.<sup>1,6</sup>

### III. COMPUTATIONAL DETAILS

DFT calculations of interacting systems are effectively limited by the computational challenge of accurately calculating the kinetic energy, a step which requires solving the noninteracting particle Schrödinger equation in three dimensions. One could fear that the nonlocal nature of the correlations that define the dispersive forces, i.e., the vdW-DF evaluation of the  $E_c^{\text{nl}}$ , may also represent a computational challenge for large systems. However, efficient algorithms are now in place and there are, effectively, no other computational bottlenecks for biomolecular vdW-DF and/or DFT-D studies, like those presented here, than the evaluation of the (noninteracting) kinetic energy  $T_s$ .

We note that since  $E_c^{\text{nl}}$  is far less costly (for large systems) than any calculation of eigenstates, it is wise to *begin* a first-principle biomolecular interaction study by mapping out the  $E_c^{\text{nl}}$  variation; this saves the costly determination of the kinetic-energy repulsion to relevant interaction morphologies. Here we pursue this first mapping step of evaluating  $E_c^{\text{nl}}$  to identify optimal DNA-dimer configurations. We also characterize the sensitivity of the vdW binding to variations in alignment of DNA structural motifs.

Figure 2 illustrates our process in our  $E_c^{\text{nl}}$ -mapping. It is formally the first step in an overall Harris-type approach for an accelerated vdW-DF evaluation of intermolecular interactions.<sup>18</sup>

The DNA-dimer electron density  $n_d$  is needed for evaluating  $E_c^{\text{nl}}[n_d]$  for the dimer. For the individual DNA we

calculate the electron density in a Linear Combination of Atomic Orbitals (LCAO) characterization, available in the DFT code GPAW.<sup>41</sup> As an approximation of  $n_d$  we use the superposition

$$n_d(\mathbf{r}) = n_1^{\text{GGA}}(\mathbf{r}) + n_2^{\text{GGA}}(\mathbf{r}) \quad (1)$$

of two copies of the individual density,  $n_{1,2}^{\text{GGA}}$ . The superscript indicates a standard self-consistent GGA calculation.

The calculation of the electron density that makes up  $n_{1,2}^{\text{GGA}}$  is carried out at the  $\Gamma$  point. The length of a period along the ds-DNA is 33.8 Å, and for determining the electron density we use an orthorhombic unit cell of size  $39.5 \times 40.4 \times 33.8$  Å<sup>3</sup>. The electron density is described on a grid with a spacing of approximately 0.20 Å.

The extended system for the superposition  $n_d$  is created by first enlarging the unit cell of the individual DNA by factors  $2.3 \times 2.3 \times 1$  to obtain a unit cell of size  $90.9 \times 92.9 \times 33.8$  Å<sup>3</sup> (in Figure 2 the original unit cell is enlarged only along the first axis, for visual reasons). Then the density for the second ds-DNA is added, appropriately translated and/or rotated around the DNA axis. For rotated ds-DNA the values of the electron density on the spatial grid are interpolated from the grid values before rotation.

The set of leftmost panels of Fig. 2 summarizes this step in our vdW-DF study. By also rotating the ds-DNA densities we can map out various mutual alignments of the groove structure and study the ramifications for the vdW attractions (as described in vdW-DF or in DFT-D).

For each of the considered separations  $d$  of the dimer and for each of the relative angles of the fragments we evaluate  $E_c^{\text{nl}}$  by carrying out the integral

$$E_c^{\text{nl}}[n] = \frac{1}{2} \int n(\mathbf{r}_1) \phi[n](\mathbf{r}_1, \mathbf{r}_2) n(\mathbf{r}_2) d\mathbf{r}_1 d\mathbf{r}_2 \quad (2)$$

for the superposition density  $n_d$  of Eq. (1). Here  $\phi[n]$  is given from a tabulated kernel function, but  $\phi[n]$  still reflects the overall density variation in the interacting components.<sup>13,18,42</sup> Our code for the postprocess calculation of the  $E_c^{\text{nl}}$  value is a real-space code. For the periodicity along the DNA axes we perform the real-space evaluation step by replicating the DNA density along the  $z$  direction (the DNA axis), for a total length of up to 540 Å (depending on the need in each calculation) and then evaluate (2) with one spatial coordinate restricted to the central unit cell, as described in Ref. 17 and illustrated also in Ref. 43. This is indicated by the right panel of Fig. 2

The ds-DNA structure can be roughly approximated by a CNT-like cylindrical structure (although filled) when viewed at large wall-to-wall separation. For a comparison we present CNT calculations using a (15,15) CNT with the electron density (of the individual CNT) obtained in a  $40.7 \times 40.7 \times 2.46$  Å<sup>3</sup> unit cell that contains 60 atoms. The radius of the (15,15) CNT is  $\langle r \rangle_{\text{CNT}} = 10.0$  Å, approximately the size of the DNA radius. For the CNT

we have chosen to use the GPAW finite differences mode (instead of LCAO) as a basis for the individual CNT electron density variation. We also set a grid for the description of the electron density that has a spacing less than 0.135 Å between grid points, and we use a Monkhorst-Pack  $k$ -point sampling of the Brillouin zone with a  $1 \times 1 \times 16$  mesh. Like for the DNA dimer, the CNT dimer density is obtained as a superposition of the individual densities.

In an additional set of comparisons, we also report DFT-D2 calculations of the vdW attraction for dimers of DNA and for dimers of CNTs. These are based on the dimer atomic configurations. The DFT-D calculations are carried out as follows. For each of the DNA/CNT atoms in the original unit cell, we sum the pair contributions over atoms in the repeated copies of the DNA or CNT unit cell, with the repetitions extending over 473 Å (or 8890 atoms) for the DNA-dimer problem and over 404 Å (or 9900 atoms) for the CNT-dimer problem.

## IV. RESULTS AND DISCUSSION

### A. A mapping of mutual vdW attraction in a soft twinning of two B-DNA coils

We first explore the vdW sensitivity of the DNA interactions as one DNA is rotated (rigidly) around another DNA, as illustrated in the insert of Fig. 3. In the rotation  $\theta$  the individual DNA is not rotated around its own axis. Instead the situation corresponds to keeping the DNA dimer axes fixed in space and rotating the left hand side DNA by the angle  $-\theta$  around its own axis while simultaneously rotating the right hand side DNA around its own axis by the angle  $-\theta$ . Effectively we are thus exploring what variation arises in the vdW attraction effects when twinning the two B-DNA coils. We restrict this twinning to situations that create no significant density overlap.

Each of the curves in Fig. 3 corresponds to a certain relative twinning rotation  $\theta$  and shows the interaction  $E_c^{\text{nl}}$  at various dimer separations (wall-to-wall distance  $\Delta$  or center-to-center distance  $d$ ) from values smaller than expected at the dimer binding,  $\Delta = 2.94$  Å, and up to  $\Delta = 12.4$  Å.

We note that the value of  $E_c^{\text{nl}}$  varies strongly with wall-to-wall separation  $\Delta$ , but except at the very small separation  $\Delta = 2.94$  Å, the order of the curves of largest and smallest contribution remain the same.

We cover the variation in the rotation angle  $\theta$  up to 90° with steps of 10°, and we find variation in the DNA vdW binding  $\theta$ . At about  $\Delta = 3.7$  Å (within binding-distance range) the variation, per unit length, in  $E_c^{\text{nl}}$  with  $\theta$  amounts to about 7 meV/Å.

There are several local minima in the variation when viewed at fixed distance  $> 3$  Å (at  $\theta = 0^\circ$ ,  $40^\circ$ , and  $70^\circ$ ). The variation in the attraction with  $\theta$  is correlated with the alignment of the grooves, but the presence of several local minima also shows that detailed structure in the

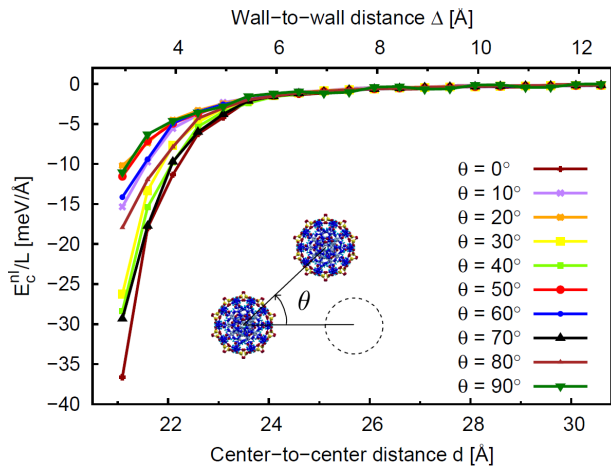


FIG. 3: Nonlocal correlation energy per length  $E_c^{nl}/L$  of the DNA dimer as a function of rotation angle  $\theta$  and separation. Both the center-to-center  $d$  and wall-to-wall distances  $\Delta$  are shown in the plot on the bottom and top horizontal axis, respectively. The picture in the insert shows the geometry of the system as the angle  $\theta$  is varied.

DNA further influences the interaction. For example, the DNA is not a continuous double helix, but consists of a series of base pairs and the associated parts of the backbone, at 3.4 Å apart along the DNA axis, and the choice of bases in the base pairs varies along the DNA. Thus we should not expect smooth, largely monotonous curves when the relative orientations of the DNA fragments are changed.

### B. Interaction effects by the alignment of motifs

The curves in Figure 3 show significant variation in  $E_c^{nl}$  with relative orientation of the DNA fragments. We therefore further explore the sensitivity to alignment of structural motifs by keeping one of the two DNA fragments fixed and rotating the other by an angle  $\phi$ . Our study creates a 360° mapping of  $E_c^{nl}/L$  versus  $\phi$ , the rotation of one B-DNA coil. The results are shown in Figure 4. The interaction is evaluated at a separation  $\Delta = 4.5$  Å which is slightly larger than the expected binding distance. At closer distances some orientations will result in overlap of high densities at the outer O atoms on the two fragments (because DNA is not truly cylindrical).

Fig. 4 demonstrates a significant and rapid variation of the vdW binding with the alignment of motifs, i.e., the alignment or disalignment of the major and minor grooves. There is an approximate symmetry of the nonlocal correlation energy around the central drop (at 183°), with the value  $-14.2$  meV/Å, or 12.0 meV/Å lower in energy than the least attractive orientations at that separation, namely at 125° and 235°.

The  $E_c^{nl}$  (or vdW attraction) minimum at 183° corresponds to the alignment of the two structures in a way

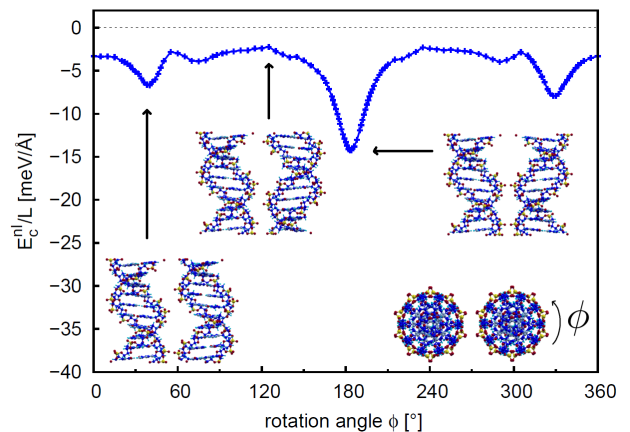


FIG. 4: The vdW binding as a function of the rotation  $\phi$  of one of the DNA molecules around its axis while keeping the other at a fixed orientation. The separation of the dimer is  $\Delta = 4.5$  Å.

that, for each of the fragments considered, two of the outermost O atoms face each other directly. This also means that the minor and major groove of the first structure are aligned with the corresponding grooves on the second DNA, as depicted in the inset picture associated to this point.

The two orientations (at  $\phi = 125^\circ$  and  $235^\circ$ ) with the largest  $E_c^{nl}/L$  values have a vdW attraction of only  $-2.4$  meV/Å, respectively  $-2.6$  meV/Å, compared to the situation of the two DNA fragments being far apart. This orientation has a large amount of vacuum between the two structures along their entire length.

Two other (minimum) features correspond to a clear enhancement in attraction, even if more modest. These local-minimum angles appear as approximately symmetric with respect to the global minimum in the  $\phi$  variation. They appear at 40° and 328° with vdW attraction  $-6.7$  meV/Å and with  $-7.9$  meV/Å. This is 4–6 meV/Å lower in energy compared to the least attractive orientation. These two local minima correspond to an alignment of the two DNA in which only one of the external O atoms faces another O atom in the other DNA.

Altogether, our vdW-DF evaluation thus makes it possible to detect variations in the nonlocal correlation energy within a  $\sim 12$  meV/Å broad range due to the alignment of the structural motifs.

### C. A comparison with vdW-extended DFT and with a CNT dimer

We continue the analysis by comparing and contrasting our vdW-DF results with results from a summation of pair contributions, using a traditional atom-based dispersive interaction form, here as provided by Grimme for the dispersion term  $D$  of DFT-D in the version DFT-D2.<sup>29</sup> Figure 5 repeats the  $\theta = 40^\circ$  and  $\theta = 50^\circ$  curves for



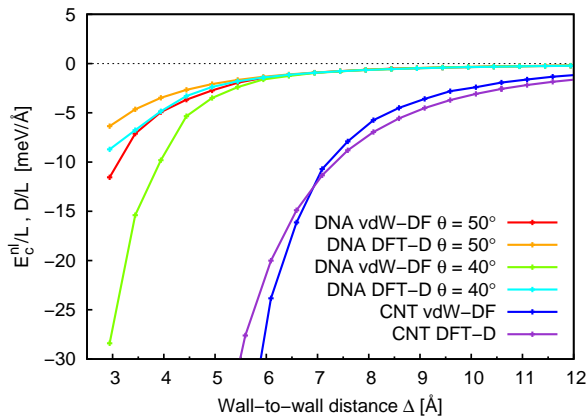


FIG. 5: DNA and CNT vdW interaction per length as a function of wall-to-wall distance  $\Delta$ .

the DNA vdW interaction and includes also the curves for the dispersion term  $D$  of DFT-D for the same two rotations.

For separations larger than about  $\Delta = 6$  Å, we find reasonable agreement between the results of the vdW-DF and DFT-D procedures (Fig. 5). At smaller separations we expect the results to differ because at close range it becomes important that the dispersion interaction arises mainly in the valence electron region, not at the atomic centers, as assumed in DFT-D. Indeed, we do see a difference in the results at small separations, with diminished attraction in the results from DFT-D compared to those from the vdW-DF method.

We also compare in Figure 5 to the attraction of a pair of parallel (15,15) CNTs that have approximately the same radius as DNA,  $\langle r \rangle_{\text{CNT}} = 10$  Å. The CNT data are calculated with vdW-DF and DFT-D. The attraction of the CNTs is stronger than for the DNA dimer. We note that there are about 30% more atoms per length (relevant for DFT-D, although also the species of the atoms matter) and more integrated electron density per length (relevant for vdW-DF) in the (15,15) CNT than in the DNA. In a previous study<sup>32,44</sup> of dimers of polyethylene (PE), polypropylene (PP), and polyvinyl chloride (PVC) two of us found a strong dependence of the vdW interaction (in a simplified method) on the integrated amount of electron charge (per length) in the polymer. In a full vdW-DF calculation, including  $E_c^{\text{nl}}$ , of PE in dimers and in a crystal, we found<sup>45</sup> the vdW term  $E_c^{\text{nl}}$  to depend strongly on the separation of the molecules and less, but not insignificantly, on the relative orientation.

We stress that there are significantly larger differences between the estimates of the vdW attraction for a CNT dimer based on our vdW-DF evaluation and the DFT-D2 evaluation, than for a DNA dimer in Fig. 6. Some of the difference must be ascribed to the difference that exists in the underlying GPAW calculation of the single-fragment electron density (a coarser-grained LCAO procedure for the DNA and a finite-different approach for

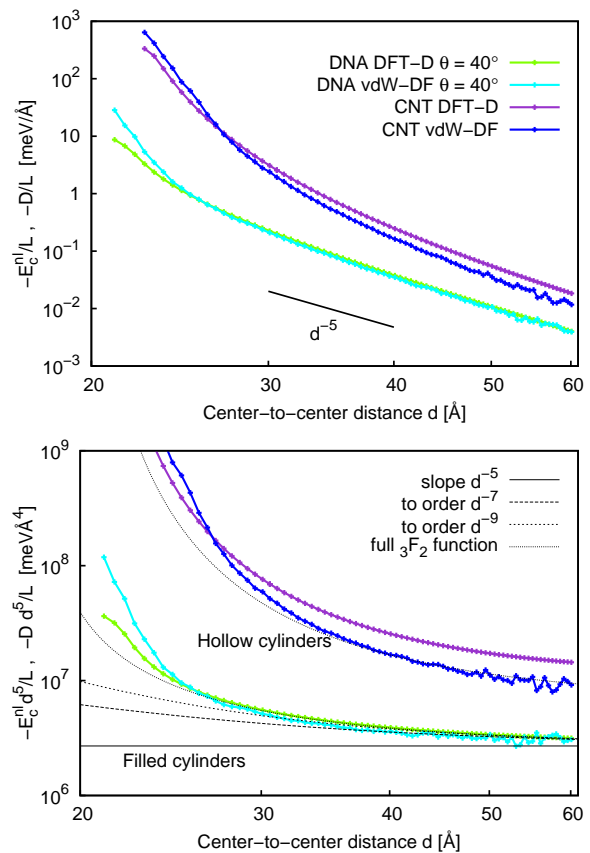


FIG. 6: The vdW interaction in DNA and CNT dimers using vdW-DF and DFT-D.

CNT). However, we expect (and are presently testing in a continuation vdW-DF study) that the differences mostly reflect the fact that for vdW-DF it is important not only how many electrons are in a molecule but also how they are distributed in space.<sup>42</sup> It is also the case that for vdW-extended DFT methods, (which use parameters to specify the per-atom contribution to the vdW interaction strength) there is now an awareness that sp<sup>2</sup>-hybridized carbon (the form that roughly applies for the CNTs) will need a different parametrization than carbon in other organic molecules (like DNA).

#### D. On the validity of a near-asymptotic interaction form

Fig. 6 analyzes the asymptotic forms of the vdW-DF and DFT-D2 results for the (15,15)-CNT and DNA interaction curves for the  $\theta = 40^\circ$  orientation. The largest center-to-center distance  $d = \Delta + 2\langle r \rangle$  is here approximately 60 Å, i.e., at the furthest separation  $d_{\text{max}}$  the ratio to the DNA radius is  $d_{\text{max}}/\langle r \rangle_{\text{DNA}} \approx 6$ . This means that only the points furthest out can possibly be considered truly asymptotic. In the asymptotic and almost-asymptotic range the  $\theta = 40^\circ$  and  $50^\circ$  curves are identi-

cal and we therefore only show the  $\theta = 40^\circ$  curves in this plot.

Beyond  $d \approx 50 \text{ \AA}$  and up to  $d_{\max}$ , which is a small range here, the interactions for the DNA and the CNT, both from vdW-DF and DFT-D calculations, scale approximately as  $-d^{-p}$  where  $p = 5$ . This is the asymptotic scaling expected for parallel cylinders. The slope of  $-d^{-5}$  is drawn in the top panel of Figure 6 as a guiding line. In general the interaction of parallel cylinders at equal radius  $b$  at large (but not necessarily asymptotic) separation  $d$  is given by the generalized hypergeometric function  ${}_3F_2$ , as described in the Appendix. This applies for cylinders of a continuous material, which our systems with atoms and varying electron distribution are not quite.

In the bottom panel of Figure 6 we plot the interaction per length, times  $d^5$ . In the truly asymptotic region for a pair of cylinders we expect a vanishing slope, and for separations a bit smaller we expect the next terms in the expansions (A.4) for filled cylinders and (A.6) for hollow cylinders to contribute. As seen in the bottom panel of Figure 6, neither the DNA nor the CNT dimers are in the fully asymptotic region at  $d < d_{\max}$  (the curves are not totally flat). However, after adding the first few terms of the expansions (A.4) or (A.6) we find good agreement with the form of the generalized hypergeometric function  ${}_3F_2$  outside the near-binding region,  $\Delta = d - 2\langle r \rangle \lesssim 4-10 \text{ \AA}$ .

Whether a pair of cylinders are filled or hollow does not affect the lowest order term in the asymptotic expansion, the  $d^{-5}$ -term. However, it does change by a factor of 2 the coefficient on the next order term, the  $d^{-7}$ -term, and thus the interaction curve in the not-quite-asymptotic region. When the DNAs or CNTs are close to each other the separation is too small for the expressions in terms of the generalized hypergeometrical functions to be valid.

It is clear that DNA is not a regular cylinder structure and that the existence of grooves must play an essential role, as also seen for the interaction as a function of relative orientation of the DNA dimer. However, far from the binding region, basing the description on an assumption of the electrons being distributed in a filled cylinder is a good approximation.

The analytical evaluation reflects the morphology of the interaction fragments and is therefore a good approximation to the pair-potential summation that underpins a DFT-D evaluation. Fig. 6 shows that the analytical description applies well as an approximation to the DFT-D results when the fragments are sufficiently removed to also make the above-stated assumptions meaningful. However, Fig. 6 also shows that our  $E_c^{\text{nl}}$ -based calculation of the vdW attraction maintains differences for the near-asymptotic form out to further distances than does the DFT-D2-based evaluation.

We ascribe these differences to the vdW-DF ability to include multipole and some collectivity effects through its plasmon-pole description<sup>13</sup> and its emphasis on reflecting the electron-density variation.<sup>16,17</sup>

## E. Towards a full vdW-DF interaction study

We note that at distances  $\Delta \lesssim 4 \text{ \AA}$  it is also important to include the remaining components of the vdW-DF method, see Ref. 16.

In a closely related study<sup>18</sup> we assess the possibility of using an adaption of the Harris scheme<sup>33-36</sup> to accelerate the evaluation also of the remaining vdW-DF (or DFT-D) components, predominantly seeking to bypass repeated evaluations of the kinetic energy variation  $T_s$ . This study shows that a high degree of accuracy can be achieved. A forthcoming paper will report the results for the DNA dimer problem and will detail effects that the DNA charging state might have on the vdW attraction.

## V. SUMMARY AND OUTLOOK

In this paper, we show that the vdW-DF functional has the potential to describe extended systems with the accuracy of DFT, thus opening a way to the description of complex soft phenomena.

We find that our computational strategy for first-principle vdW-DF characterization (with our moderate-level access to HPC) can give some qualitative and even semi-quantitative results for biomolecular systems even before the full vdW-DF (or for example DFT-D) evaluation of the kinetic-energy repulsion effects is completed.

An accelerated vdW-DF computational framework<sup>18</sup> study can be expected to work well for investigations of vdW bound systems. Here, we have illustrated the possibility of an even faster initial mapping by evaluating the vdW-binding component. An additional component in the strategy is to adapt the ideas of the Harris scheme as explored in a parallel study.<sup>18</sup> The motivation for this strategy is easily stated: even if our DNA model structure is only a model system of the full secondary genome structure, the individual ds-DNA still contains 635 atoms and the dimer system contains 1270 atoms. The size of the problem prevents us (at the supercomputing facilities to which we have access) from performing an ordinary potential-energy calculation by means of a conventional DFT implementation. More realistic studies will contain even more atoms per unit cell, or have other similar complications. Thus any computational simplification able to keep most of the original accuracy is welcome. That observation is true whether or not we wish to pursue a vdW-DF or a DFT-D study.

The nonlocal correlation energy  $E_c^{\text{nl}}$ , which contains the essential information about the vdW binding, is accessible with a limited computational effort. We have found that this  $E_c^{\text{nl}}$  evaluation has essentially perfect scaling up to at least 2000 cores in our real space implementation.<sup>17</sup>

We are thus proposing to *initialize* vdW-DF studies of large biomolecular interaction problems by first mapping out what interaction geometries are plausible, from knowing the variation in the vdW attraction. By begin-

ning the vdW-DF identification of optimal interaction geometries with this vdW-attraction step we are pursuing a course that is similar to that Nature uses in its own molecular-recognition search.

### Acknowledgments

The authors thank Professor Jason Kahn, University of Maryland, for valued discussions on the atomic coordinates in a standard idealized model of structure of a ds-DNA coil.<sup>38,39</sup> We thank Eskil Varenus and Magnus Sandén for computing a corresponding ds-B-DNA electron density that represents a starting point for the here-described mapping of the vdW attraction. Partial support from the Swedish Research Council (VR) and the Chalmers Area of Advance Materials is gratefully acknowledged. The computations were performed on resources provided by the Swedish National Infrastructure for Computing (SNIC) at C3SE and NSC.

### Appendix: Scaling of interaction at large separations

With some robust assumptions it is possible to provide analytical results for the vdW interaction per length,  $E_A/L$ , for two parallel (infinitely repeated) cylindrical structures when these are far, but not asymptotically far, apart.<sup>27,31,32</sup> The assumptions are that the matter is continuous, a slightly simplified plasmon-pole approximation, and that the (screened) effective susceptibility can be approximated as having equivalent magnitudes for response along the cylinder axis and tangent. There are some differences in this analytical evaluation for hollow (relevant for carbon nanotubes) and filled (relevant for DNA) cylinders but in both cases the results can be expressed in terms of a generalized hypergeometric function. For either types of interacting systems, we consider two cylinders of equal radius  $b$  at center-to-center distance  $d$ .

For a pair of massive cylinders a two-variable expression is given in the book by Mahanty and Ninham<sup>46,47</sup> in terms of Appells hypergeometric function  $F_4$

$$\frac{E_A^{\text{filled}}}{L} = -B \frac{b^4}{d^5} F_4 \left( \frac{5}{2}, \frac{5}{2}; 2, 2; \frac{b^2}{d^2}, \frac{b^2}{d^2} \right) \quad (\text{A.1})$$

$$= -B \frac{b^4}{d^5} \sum_{m,n=0}^{\infty} \left( \frac{\Gamma(\frac{5}{2} + m + n)}{\Gamma(\frac{5}{2})} \right)^2 \times \frac{\left(\frac{b^2}{d^2}\right)^{m+n}}{m! n! (m+1)! (n+1)!}. \quad (\text{A.2})$$

Here  $B$  is a (positive) prefactor that reflects the susceptibility of the material in the cylinders and whose value can be set by investigating the asymptotic form.

We rewrite this expression with the generalized hypergeometric function  ${}_3F_2$  of one variable

$$\frac{E_A^{\text{filled}}}{L} = -B \frac{b^4}{d^5} {}_3F_2 \left( \frac{3}{2}, \frac{5}{2}, \frac{5}{2}; 2, 3; 4 \frac{b^2}{d^2} \right). \quad (\text{A.3})$$

For large separations  $d \gg b$  an expansion in  $b/d$  yields

$${}_3F_2 \left( \frac{3}{2}, \frac{5}{2}, \frac{5}{2}; 2, 3; 4 \frac{b^2}{d^2} \right) = 1 + \frac{25}{4} \frac{b^2}{d^2} + \frac{6125}{192} \frac{b^4}{d^4} + \frac{77175}{512} \frac{b^6}{d^6} + \mathcal{O} \left( \frac{b}{d} \right)^7 \quad (\text{A.4})$$

which is the expansion used in the bottom panel of Figure 6 for the pair of DNA (approximated as filled cylinders).

For a pair of infinitely thin, hollow cylinders, where the electron density can be described by a radial  $\delta$ -function, the interaction is given by a similar generalized hypergeometric function<sup>31,32</sup>

$$\frac{E_A^{\text{hollow}}}{L} = -B \frac{b^4}{d^5} {}_3F_2 \left( \frac{1}{2}, \frac{5}{2}, \frac{5}{2}; 1, 1; 4 \frac{b^2}{d^2} \right). \quad (\text{A.5})$$

The result is also valid for a slightly more general choice of susceptibility tensors.<sup>31,32</sup> For the function (A.5) the expansion in  $b/d$  yields

$${}_3F_2 \left( \frac{1}{2}, \frac{5}{2}, \frac{5}{2}; 1, 1; 4 \frac{b^2}{d^2} \right) = 1 + \frac{25}{2} \frac{b^2}{d^2} + \frac{3675}{32} \frac{b^4}{d^4} + \frac{55125}{64} \frac{b^6}{d^6} + \mathcal{O} \left( \frac{b}{d} \right)^7 \quad (\text{A.6})$$

This expansion is used in the bottom panel of Figure 6 for the pair of CNT (approximated as pipes, that is, hollow cylinders).

\* Electronic address: schroder@chalmers.se; Corresponding author

<sup>1</sup> E. Schrödinger, *What is life?* (Cambridge University Press, Cambridge, 1967).



- <sup>2</sup> J.D. Watson and F.H.C. Crick, *Nature* **171**, 4356 (1953).
- <sup>3</sup> H.M. Berman, W.K. Olson, D.L. Beveridge, J. Westbrook, A. Gelbin, T. Demeny, S.-H. Hsieh, A.R. Srinivasan, and B. Schneider, *Biophys. J.* **63**, 751 (1992); <http://ndbserver.rutgers.edu>
- <sup>4</sup> M.C. Williams, L. J. Maher III, eds., “Biophysics of DNA-Protein Interactions” (Springer, New York, 2011).
- <sup>5</sup> A.L. Lehninger, D.L. Nelson, and M.M. Cox, *Principles of Biochemistry*, (Worth Publishers, Inc., New York, 1993).
- <sup>6</sup> For example, S.H. Gellman, *Chem. Rev.* **97**, 1231 (1997) and associated collected reviews in *Chem. Rev.* **97**; P.J. Edmonson *et al.*, *Int. J. Mod. Sci.* **9**, 154 (2008).
- <sup>7</sup> V.R. Cooper, T. Thonhauser, A. Puzder, E. Schröder, B.I. Lundqvist, and D.C. Langreth, *J. Amer. Chem. Soc.* **130**, 1304 (2008).
- <sup>8</sup> S. Li, V.R. Cooper, T. Thonhauser, B.I. Lundqvist, and D.C. Langreth, *J. Phys. Chem. B* **113**, 11166 (2009).
- <sup>9</sup> K. Burke, *J. Chem. Phys.* **136**, 150901 (2012).
- <sup>10</sup> H. Rydberg, N. Jacobson, P. Hyldgaard, S.I. Simak, B.I. Lundqvist, and D.C. Langreth, *Surf. Sci.* **532–535**, 606 (2003).
- <sup>11</sup> D.C. Langreth, M. Dion, H. Rydberg, E. Schröder, P. Hyldgaard, and B.I. Lundqvist, *Intern. J. Quant. Chem.* **101**, 599 (2005).
- <sup>12</sup> D.C. Langreth, B.I. Lundqvist, S.D. Chakarova-Käck, V.R. Cooper, M. Dion, P. Hyldgaard, A. Kelkkanen, J. Kleis, L. Kong, S. Li, P.G. Moses, E. Murray, A. Puzder, H. Rydberg, E. Schröder, and T. Thonhauser, *J. Phys.: Cond. Matter* **21**, 084203 (2009).
- <sup>13</sup> M. Dion, H. Rydberg, E. Schröder, D.C. Langreth, and B.I. Lundqvist, *Phys. Rev. Lett.* **92**, 246401 (2004); **95**, 109902(E) (2005).
- <sup>14</sup> T. Thonhauser, V.R. Cooper, S. Li, A. Puzder, P. Hyldgaard, and D.C. Langreth, *Phys. Rev. B* **76**, 125112 (2007).
- <sup>15</sup> K. Lee, E.D. Murray, L. Kong, B.I. Lundqvist, and D.C. Langreth, *Phys. Rev. B* **82**, 081101(R) (2010).
- <sup>16</sup> K. Berland and P. Hyldgaard, *J. Chem. Phys.* **132**, 134705 (2010).
- <sup>17</sup> K. Berland, Ø. Borck, and P. Hyldgaard, *Comp. Phys. Commun.* **182**, 1800 (2011).
- <sup>18</sup> K. Berland, E. Londero, E. Schröder, and P. Hyldgaard, *A Harris-type van der Waals density functional scheme*, arXiv:1303.3762 [cond-mat.mtrl-sci].
- <sup>19</sup> Y.U. Barash, *Fiz. Tverd. Tela.* **30**, 1578 (1988); B. E. Sernelius and P. Björk, *Phys. Rev. B* **57**, 6592 (1998).
- <sup>20</sup> J. F. Dobson and T. Gould, *J. Phys.: Condens. Matter* **24**, 073201 (2012); S. Lebégue, J. Harl, T. Gould, J. Ángyán, G. Kresse, and J.F. Dobson, *Phys. Rev. Lett.* **105**, 196401 (2010).
- <sup>21</sup> J.P. Perdew, J. Tao, P. Hao, A. Ruzsinszky, G.I. Csonka, and J.M. Pitarke, *J. Phys.: Condens. Matter* **24**, 424207 (2012); A. Ruzsinszky, J.P. Perdew, J. Tao, G.I. Csonka, and J. M. Pitarke, *Phys. Rev. Lett.* **109**, 233203 (2012).
- <sup>22</sup> G. Román-Pérez and J.M. Soler, *Phys. Rev. Lett.* **103**, 096102 (2009).
- <sup>23</sup> E. Ziambaras, J. Kleis, E. Schröder, and P. Hyldgaard, *Phys. Rev. B* **76**, 155425 (2007).
- <sup>24</sup> A. Gulans, M.J. Puska, and R.M. Nieminen, *Phys. Rev. B* **79**, 201105(R) (2009).
- <sup>25</sup> D. Nabok, P. Puschnig, C. Ambrosch-Draxl, *Comp. Phys. Commun.* **182**, 1657 (2011).
- <sup>26</sup> Open-source tool JuNoLo for real-space and fast-fourier transform non-selfconsistent vdW-DF total-energy evaluation; P. Lazić, N. Atodiresei, M. Alaei, V. Caciuc, S. Blügel, and R. Brako, *Comp. Phys. Comm.* **181**, 371 (2010).
- <sup>27</sup> J. Kleis, E. Schröder, and P. Hyldgaard, *Phys. Rev. B* **77**, 205422 (2008).
- <sup>28</sup> X. Wu, M.C. Vargas, S. Nayak, V. Lotrich, and G. Scoles, *J. Chem. Phys.* **115**, 8748 (2001); S. Grimme, *J. Comp. Chem.* **25**, 1463 (2004).
- <sup>29</sup> S. Grimme, *J. Comp. Chem.* **27**, 1787 (2006).
- <sup>30</sup> E. Schröder and P. Hyldgaard, *Surf. Sci.* **532**, 880 (2003).
- <sup>31</sup> E. Schröder and P. Hyldgaard, *Mater. Sci. Engin. C* **23**, 721 (2003).
- <sup>32</sup> J. Kleis, P. Hyldgaard, and E. Schröder, *Comp. Mater. Sci.* **33**, 192 (2005).
- <sup>33</sup> J. Harris, *Phys. Rev. B* **31**, 1770 (1985).
- <sup>34</sup> W.M.C. Foulkes and R. Haydock, *Phys. Rev. B* **39**, 12520 (1989).
- <sup>35</sup> V.K. Nikulin, *Zh. Tekhn. Fiz.* **XLI**, 41 (1971) [*Sov. Phys. - Techn. Phys.* **16**, 28 (1971)].
- <sup>36</sup> R.G. Gordon and Y.S. Kim, *J. Chem. Phys.* **56**, 3122 (1972).
- <sup>37</sup> A. Kokalj, *Comp. Mater. Sci.* **28**, 155 (2003). Code available from <http://www.xcrysden.org/>
- <sup>38</sup> S. Arnott and D.W.L. Hukins, *Biochem. Biophys. Research Commun.* **47**, 1504 (1972).
- <sup>39</sup> S. Arnott, D.W.L. Hukins, and S.D. Dover, *Biochem. Biophys. Research Commun.* **48**, 1392 (1972).
- <sup>40</sup> The idealized atomic coordinates for the here-investigated base-pair sequence in our infinitely repeated ds-DNA model system were put together by Prof. Jason Kahn, University of Maryland. The coordinates are available as part of his instructive rasmol tutorial, available at [http://www.biochem.umd.edu/biochem/kahn/teach\\_res](http://www.biochem.umd.edu/biochem/kahn/teach_res)
- <sup>41</sup> Open-source, grid-based PAW-method DFT code GPAW, <http://wiki.fysik.dtu.dk/gpaw/>
- <sup>42</sup> K. Berland and P. Hyldgaard, *An analysis of van der Waals density functional components: Binding and corrugation of benzene and C60 on boron nitride and graphene*, arXiv:1303.0389 [cond-mat.mes-hall].
- <sup>43</sup> K. Berland, S.D. Chakarova-Käck, V.R. Cooper, D.C. Langreth, and E. Schröder, *J. Phys.: Cond. Matter* **23**, 135001 (2011).
- <sup>44</sup> J. Kleis and E. Schröder, *J. Chem. Phys.* **122**, 164902 (2005).
- <sup>45</sup> J. Kleis, B.I. Lundqvist, D.C. Langreth, and E. Schröder, *Phys. Rev. B* **76**, 100201(R) (2007).
- <sup>46</sup> J. Mahanty and B.W. Ninham, *Dispersion Forces* (Academic Press, London, 1976).
- <sup>47</sup> Please note that there is a typographical error in Ref. 46 in what corresponds to the last expression below.